

## Zn<sup>2+</sup> Slows Down Ca<sub>v</sub>3.3 Gating Kinetics: Implications for Thalamocortical Activity

M. Cataldi,<sup>1</sup> V. Lariccia,<sup>1</sup> V. Marzaioli,<sup>1</sup> A. Cavaccini,<sup>1</sup> G. Curia,<sup>2</sup> D. Viggiano,<sup>1</sup> L.M.T. Canzoniero,<sup>1</sup> G. di Renzo,<sup>1</sup> M. Avoli,<sup>2,3</sup> and L. Annunziato<sup>1</sup>

<sup>1</sup>Divisione di Farmacologia, Dipartimento di Neuroscienze, Facoltà di Medicina e Chirurgia, Università di Napoli Federico II, Naples, Italy; <sup>2</sup>Montreal Neurological Institute and Department of Neurology and Neurosurgery, McGill University, Montreal, Quebec, Canada; and <sup>3</sup>Dipartimento di Medicina Sperimentale, Prima Facoltà di Medicina e Chirurgia, Università di Roma Sapienza, Rome, Italy

Submitted 21 August 2006; accepted in final form 15 August 2007

**Cataldi M, Lariccia V, Marzaioli V, Cavaccini A, Curia G, Viggiano D, Canzoniero LM, di Renzo G, Avoli M, Annunziato L.** Zn<sup>2+</sup> slows down Ca<sub>v</sub>3.3 gating kinetics: implications for thalamocortical activity. *J Neurophysiol* 98: 2274–2284, 2007. First published August 15, 2007; doi:10.1152/jn.00889.2006. We employed whole cell patch-clamp recordings to establish the effect of Zn<sup>2+</sup> on the gating the brain specific, T-type channel isoform Ca<sub>v</sub>3.3 expressed in HEK-293 cells. Zn<sup>2+</sup> (300 μM) modified the gating kinetics of this channel without influencing its steady-state properties. When inward Ca<sup>2+</sup> currents were elicited by step depolarizations at voltages above the threshold for channel opening, current inactivation was significantly slowed down while current activation was moderately affected. In addition, Zn<sup>2+</sup> slowed down channel deactivation but channel recovery from inactivation was only modestly changed. Zn<sup>2+</sup> also decreased whole cell Ca<sup>2+</sup> permeability to 45% of control values. In the presence of Zn<sup>2+</sup>, Ca<sup>2+</sup> currents evoked by mock action potentials were more persistent than in its absence. Furthermore, computer simulation of action potential generation in thalamic reticular cells performed to model the gating effect of Zn<sup>2+</sup> on T-type channels (while leaving the kinetic parameters of voltage-gated Na<sup>+</sup> and K<sup>+</sup> unchanged) revealed that Zn<sup>2+</sup> increased the frequency and the duration of burst firing, which is known to depend on T-type channel activity. In line with this finding, we discovered that chelation of endogenous Zn<sup>2+</sup> decreased the frequency of occurrence of ictal-like epileptiform discharges in rat thalamocortical slices perfused with medium containing the convulsant 4-aminopyridine (50 μM). These data demonstrate that Zn<sup>2+</sup> modulates Ca<sub>v</sub>3.3 channel gating thus leading to increased neuronal excitability. We also propose that endogenous Zn<sup>2+</sup> may have a role in controlling thalamocortical oscillations.

### INTRODUCTION

T-type channels—which possess peculiar kinetic properties along with differences in ionic permeation when compared with high-voltage activated Ca<sup>2+</sup> channels (Cataldi et al. 2002; Tsien et al. 1988)—are crucial in regulating the periodic discharge of cells in relay thalamic nuclei and in nucleus reticularis thalami (nRT). These neurons are an integral component of the thalamocortical system that is known to be involved in physiological and pathological conditions such as absence epilepsy (Destexhe and Sejnowski 2003; Perez-Reyes 2003; Steriade 2005; Steriade et al. 1993).

At least three different T-type channel isoforms are expressed in neurons as well as in different compartments of the

same neuron (Joksovic et al. 2005a; Talley et al. 1999). These include Ca<sub>v</sub>3.1 (Perez-Reyes et al. 1998) and Ca<sub>v</sub>3.2 (Cribbs et al. 1998) channels—which carry the classical fast inactivating T-type current (Carbone and Lux 1984; Fox et al. 1987; Kostyuk et al. 1988)—and the Ca<sub>v</sub>3.3 channels (Lee et al. 1999), carrying more slowly inactivating currents such as those recorded in nRT cells (Huguenard and Prince 1992). As these different isoforms have specific kinetic properties, neuron behavior will depend on the type of T-current it expresses. Specifically, because slow inactivating Ca<sub>v</sub>3.3 channels are required to fire action potentials at a high frequency and for prolonged periods of time (Kozlov et al. 1999), their presence in nRT cells may be essential for periodic spiking (Destexhe and Sejnowski 2003).

Although point mutations affecting channel gating have been identified in absence epilepsy (Khosravani et al. 2004; Vitko et al. 2005), it is unknown how endogenous neurotransmitters or neuromodulators influence T-type-dependent spiking. Here we explore the hypothesis that Ca<sub>v</sub>3.3 channel gating could be affected by Zn<sup>2+</sup>, which is stored with glutamate in the terminals of a subset of cells, also called the *gluzinergic neurons*, and coreleased with this excitatory neurotransmitter (Frederickson et al. 2000, 2005; Howell et al. 1984; Qian and Noebels 2005). That Zn<sup>2+</sup> may affect T-type channel gating is suggested by the evidence that this metal does affect the gating kinetics of other voltage-gated ion channels (Harrison and Gibbons 1994; Mathie et al. 2006) and greatly increases neuronal excitability in the thalamus, thus suggesting its involvement in absence epilepsy (Gibbs et al. 2000; Wu et al. 2004). Therefore we explored here the hypothesis that Zn<sup>2+</sup> influences the slowly inactivating T-type current expressed in nRT neurons—which is encoded by the Ca<sub>v</sub>3.3 gene (Talley et al. 1999)—by evaluating the effects of exogenous Zn<sup>2+</sup> on Ca<sub>v</sub>3.3 channels heterologously expressed in stably transfected HEK-293 cells as their currents are identical to those recorded in nRT neurons (Joksovic et al. 2005b). This experimental approach allows study of this channel type in isolation without any interference from other ion channels. By doing so, we found that this ion slowed down the gating of Ca<sub>v</sub>3.3 channel heterologously expressed in HEK-293 cells. We also discovered that when the changes in gating were translated into simulated nRT neurons by using the NEURON software interface (Hines and Carnevale 1997), the frequency and duration

Address for reprint requests and other correspondence: L. Annunziato, Div. di Farmacologia, Dipt. di Neuroscienze, Via Pansini 5, 80131 Napoli, Italy (E-mail: lannunzi@unina.it).

The costs of publication of this article were defrayed in part by the payment of page charges. The article must therefore be hereby marked “advertisement” in accordance with 18 U.S.C. Section 1734 solely to indicate this fact.

of T-type-dependent action potential trains increased. Finally, we established in rat thalamocortical slices maintained in vitro that chelating endogenous Zn<sup>2+</sup> decreased the frequency of occurrence of ictal-like epileptiform discharges generated in the presence of the K<sup>+</sup> channel blocker 4-aminopyridine (4AP).

## METHODS

### Cell culture

Stably transfected HEK-293 cells (courtesy of Dr. Perez-Reyes), expressing the rat Ca<sub>v</sub>3.3a T-type Ca<sup>2+</sup> channel isoform (Ca<sub>v</sub>3.3 cells) (Lee et al. 1999), were cultured in a humidified 5% CO<sub>2</sub> atmosphere using Dulbecco's modified Eagle's medium supplemented with 5% fetal calf serum, 100 IU/ml penicillin, 100 μg/ml streptomycin, and nonessential amino acids; they were kept under constant selection with 1 g/l geneticin. For electrophysiological recordings, cells were plated on poly-L-lysine (30 μg/ml) precoated glass coverslips and used 24–48 h after plating.

### Whole cell patch-clamp recordings

Experiments were performed using the whole cell configuration of the patch-clamp technique as previously reported (Cataldi et al. 2004). Briefly, the coverslips used for cell culture were placed into a laminar flow chamber (Warner Instrument, Hamden, CT) mounted on the stage of a Axiovert 25 Zeiss inverted microscope. The cells were continuously superfused by a gravity-fed multilane system controlled by microcomputer-operated electro-valves (Cell Micro-control, Norfolk, VA) that allowed the rapid exchange of the perfusing solution. Whole cell recordings were performed at room temperature (25–26°C).

Ruptured patches were obtained by suction using fire-polished borosilicate electrodes having a final resistance of 3–5 MΩ and back filled with a CsCl-based internal solution containing (in mM) 110 CsCl, 30 tetraethyl ammonium chloride (TEA-Cl), 10 EGTA, 2 MgCl<sub>2</sub>, 10 HEPES, 8 glucose, 15 phosphocreatine di-sodium salt, 5 ATP di-sodium salt, and 1 cAMP sodium salt (pH 7.4 adjusted with CsOH). Unless otherwise specified, the external solution contained (in mM) 125 N-methyl-D-glucamine (NMDG), 2 CaCl<sub>2</sub>, 1 MgCl<sub>2</sub>, 5 CsCl, 10 glucose, and 10 HEPES (pH 7.4 adjusted with HCl, yielding a final Cl<sup>-</sup> concentration of ~110 mM, as determined by silver nitrate titration). Under these experimental conditions, Ca<sup>2+</sup> currents are presumably recorded in isolation because K<sup>+</sup> currents are blocked by CsCl present in both internal and external solution and by TEA-Cl contained in the internal solution; in addition, no detectable Na<sup>+</sup> current is expected to flow through the membrane because of the lack of Na<sup>+</sup> channels in HEK-293 cells and because of the substitution of external Na<sup>+</sup> with NMDG. The osmolarity of the external solution was adjusted to 300 mosM by adding an appropriate amount of sucrose. All the voltages reported in the text or shown in figures represent the values obtained after correction for junction potential (~7 mV in accordance with the estimate provided by the junction potential calculator included in the pClamp8 software) and charge screening (~4 mV).

Test pulses were generated and the ensuing currents were collected with an Axon 200 B patch-clamp amplifier (Molecular Devices, Foster City, CA) driven by the pClamp6 software running on a personal computer. Currents were filtered at 2 kHz with the amplifier built-in Bessel filter, and leak currents were subtracted on-line with a P/4 protocol. Using the specific commands of the amplifier, on-line correction of membrane capacitance and series resistance was routinely performed. Data were stored onto the hard disk of the personal computer. Off-line analyses were then performed with the Clampfit 8.0 (Molecular Devices) and Sigmaplot 5.0 (SPSS, Chicago, IL) softwares.

### Patch-clamp data analysis and computer modeling

The voltage-dependence of activation constants,  $V_{1/2m}$  (the membrane potential at which the current is half-maximal) and  $k_m$  (the voltage required to change the conductance,  $g$ ,  $e$ -fold), were calculated fitting the  $I$ - $V$  data to the Goldman and Hodgkin current equation as reported by McCormick and Huguenard (1992)

$$I_{Ca} = \hat{g} P z^2 \frac{VF^2 [Ca^{2+}]_i - [Ca^{2+}]_o \exp(-zFV/RT)}{RT (1 - \exp(-zFV/RT))} \quad (1)$$

where  $I_{Ca}$  is the current carried by Ca<sup>2+</sup> ions (in A)  $P$  is the maximum permeability in cm<sup>3</sup>/s,  $z$  is 2 (the valence of Ca<sup>2+</sup>),  $V$  is the applied voltage in V,  $F$  is the Faraday constant,  $R$  is the gas constant,  $T$  is the absolute temperature in Kelvin degrees and  $\hat{g}$  represents fractional conductance

$$\hat{g} = G/G_{max} \quad (2)$$

Because

$$\frac{G}{G_{max}} = \frac{1}{1 + \exp((V_{1/2m} - V)/k_m)} \quad (3)$$

for fitting purposes, Eq. 2 was expressed in the form

$$I_{Ca} = P z^2 \frac{VF^2 [Ca^{2+}]_i - [Ca^{2+}]_o \exp(-zFV/RT)}{RT (1 - \exp(-zFV/RT))} \frac{1}{1 + \exp((V_{1/2m} - V)/k_m)} \quad (4)$$

The values of activation ( $\tau_m$ ) and inactivation time constants ( $\tau_h$ ) of the inward Ca<sup>2+</sup> currents evoked by membrane depolarization to suprathreshold voltages were obtained by fitting current data to the Hodgkin and Huxley equation

$$I_{Ca} = g_{Ca} * m^2 * h * (V - E_{Ca}) \quad (5)$$

where  $V$  is the applied voltage,  $E_{Ca}$  is the reversal potential of Ca<sup>2+</sup> currents, and the fraction of open activation ( $m$ ) and inactivation ( $h$ ) gates are calculated from the relations

$$\frac{dm}{dt} = \frac{m^\infty(V) - m}{\tau_m(V)} \quad (6)$$

$$\frac{dh}{dt} = \frac{h^\infty(V) - h}{\tau_h(V)} \quad (7)$$

and

$$m^\infty(V) = \frac{1}{1 + \exp((V - V_{1/2m})/k_m)} \quad (8)$$

$$h^\infty(V) = \frac{1}{1 + \exp((V - V_{1/2h})/k_h)} \quad (9)$$

where  $V_{1/2m}$  and  $V_{1/2h}$  are respectively the half-voltage of activation and of inactivation and  $k_m$  and  $k_h$  are the slopes respectively of activation and inactivation.

Data fitting was performed using the NEUROFIT software (developed by Allan Willms, Gregory Ewing, and Howie Kuo at the Department of Mathematics and Statistics of the University of Guelph, Guelph, Canada and freely downloadable at the internet address [www.uoguelph.ca/~awillms/neurofit/](http://www.uoguelph.ca/~awillms/neurofit/)). Tail currents appearing during channel deactivation were fitted to a bi-exponential equation with fast ( $\tau_1$ ) and slow ( $\tau_2$ ) time constants. For fitting purposes, the kinetics of tail relaxation was expressed by the single kinetic parameter  $\tau$  weighted ( $\tau_w$ ) that was calculated using the equation

$$\tau_w = A1 * \tau_1 + A2 * \tau_2 \quad (10)$$

where  $A1$  and  $A2$  represent the relative amplitude of the fast ( $A_1$ ) and of the slow ( $A_2$ ) decay component of the tail current.

Simulations of current-clamp recordings in modeled reticular thalamic cells were performed using the NEURON 5.8 software (Hines and Carnevale 1997), freely downloadable at [www.neuron.yale.edu/neuron](http://www.neuron.yale.edu/neuron). The IT2 model file required to run the NEURON simulation was obtained by entering the kinetics parameters—obtained from the experiments described in the results section—into the model file developed by Murbartian et al. (2004), which was kindly provided by Dr. E. Perez-Reyes (Department of Pharmacology, University of Virginia, Charlottesville, VA). This *mod* file used for  $\text{Ca}_v3.3$  cells is a modified version of the model file originally developed by Destexhe et al. (1996) for thalamic reticular cells (downloadable at Dr. Destexhe web site, <http://cns.iaf.cnrs-gif.fr/Main.html>). The NEURON software extrapolates the changes in membrane voltage evoked by the injection of current into the cells by applying an  $m^2$  Hodgkin Huxley formalism according to Eq. 5. To get this software running, the fitting parameters needed to calculate  $m^\infty$  and  $h^\infty$ , and the kinetic constants  $\tau_m$  and  $\tau_h$  have to be entered into the program. The values of the kinetic constants of activation ( $V_{1/2m}$  and  $k_m$ ) were obtained fitting the  $I$ - $V$  data to the Goldman and Hodgkin current equation as described in the preceding text, whereas those for inactivation ( $V_{1/2h}$  and  $k_h$ ) were obtained by fitting the steady-state inactivation data to the Boltzmann equation

$$I = \frac{I_{\max}}{1 + \exp((V_{1/2h} - V)/k_h)} \quad (11)$$

Both the voltage dependence of the activation time constant ( $\tau_m$ ) and that of the inactivation time constant ( $\tau_h$ ) were specified by the equation

$$\tau = (C + 1.0/\{\exp[(V + V_1)/k_1] + \exp[-(V + V_2)/k_2]\}) \quad (12)$$

where  $V_1$ ,  $V_2$  and  $k_1$ ,  $k_2$  represent the half-voltages ( $V_{1/2}$ ) and slopes of increasing and decreasing components of the bell shaped curves generated by plotting  $\tau_m$  or  $\tau_h$  data obtained at the different tested voltages as detailed in RESULTS.

Using Eq. 5, the NEURON software calculates  $I_{\text{Ca}}$  as a function of  $\text{Ca}^{2+}$  conductance  $g_{\text{Ca}}$  (5). In our simulation of nRT neurons bathed with 2 mM  $\text{Ca}^{2+}$  and no  $\text{Zn}^{2+}$ , we used the  $g_{\text{Ca}}$  value of 0.0008 (Siemens/cm<sup>2</sup>) reported in the original nRT model developed by Destexhe et al. (1996) and adapted to HEK cells by Murbartian et al. (2004). Conversely, when the addition of  $\text{Zn}^{2+}$  was simulated, to reproduce the 55% decrease in  $\text{Ca}^{2+}$  permeability that we observed in our whole cell recordings, we lowered the above-reported  $g_{\text{Ca}}$  value by introducing a multiplication factor of 0.455, according to the equation

$$I_{\text{Ca}} = 0.455 * g_{\text{Ca}} * m^2 * h * (V - E_{\text{Ca}}) \quad (13)$$

The entire simulation was run using the option “burst behavior in a three-compartment model” keeping the resting potential at  $-70$  mV, a value close to those observed in thalamic neurons *in vivo* during sleep (Fuentelba et al. 2005).

### Field potential recordings in talamocortical slices

Thalamocortical slices were obtained using the modifications proposed by Biagini et al. (2001) of the original procedures described by Agmon and Connor (1991). Procedures were approved by the Canadian Council of Animal Care. Briefly young male Sprague-Dawley rats (15–28 days old) were deeply anesthetized with isoflurane and killed by decapitation. The skull was quickly opened, and the brain was removed, placed into an ice-cold oxygenated sucrose-containing solution (in mM: 206 sucrose, 3.5 KCl, 1  $\text{CaCl}_2$ , 2  $\text{MgSO}_4$ , 1.25  $\text{NaH}_2\text{PO}_4$ , 26  $\text{NaHCO}_3$ , 1  $\text{MgCl}_2$ , 10 glucose, 0.4 ascorbic acid, and 1 kynurenic acid) and left to refrigerate into this solution for 3–4 min. Then the brain was transferred onto a Plexiglas ramp the surface of which makes a  $10^\circ$  angle with the horizontal plane. Brain stem

and cerebellum were removed with a razor blade by a vertical cut. Then the frontal pole was vertically cut along a plane describing a  $45^\circ$  angle with the sagittal plane. During the entire procedure, the brain was repeatedly irrigated with ice-cold cutting solution. The cut surface of the frontal pole was glued onto the chamber of a Leica VT1000S vibratome (Richmond Hill, Ontario, Canada). Then this chamber was filled with an ice-cold cutting solution, which was continuously oxygenated via an oxygen line, and the brain was cut in  $450\text{-}\mu\text{m}$ -thick slices. Only the slices clearly showing bundles of fibers connecting cortex and thalamus were chosen for electrophysiological recordings. On average three to four slices per animal showed these characteristics. Chosen slices were transferred onto the surface of a custom-made interface perfusion chamber and let equilibrate for 1–1.5 h while continuously superfused with oxygenated artificial cerebrospinal fluid (ACSF) (containing in mM: 124 NaCl, 2 KCl, 1.25  $\text{KH}_2\text{PO}_4$ , 0.5  $\text{MgSO}_4$ , 2  $\text{CaCl}_2$ , 26  $\text{NaHCO}_3$ , and 10 glucose) at  $32^\circ\text{C}$ . At the end of this equilibration period, the  $\text{K}^+$  channel blocker 4AP (50  $\mu\text{M}$ ) was added to the medium to induce spontaneous epileptiform activity (Biagini et al. 2001), and the slices were perfused with this 4AP containing ACSF for an additional hour. ACSF-filled borosilicate electrodes (resistance =  $\sim 10$  M $\Omega$ ) were placed under visual control with the help of a stereomicroscope into the parietal cortex, the ventrobasal nucleus (VB) of the thalamus and the nRT. Field potentials were recorded with preamplifier probes connected with a Cyber-amp 300 signal conditioner (Axon Instruments, Molecular Devices), digitized at 5 kHz with a Digidata 1200 A/D converter and stored as pClamp8 files (Axon Instruments, Molecular Devices) for off-line analysis. After recording the baseline activity for  $>30$  min, the cell membrane-permeant  $\text{Zn}^{2+}$  chelator *N,N,N',N'*-tetrakis(2-pyridylmethyl) ethylenediamine (TPEN) was added to the solution and data were recorded in the presence of this drug for additional 30–45 min. Finally, TPEN was washed out and data were acquired for 30 more min. Data analysis was performed off-line with the Clampfit 8 software (Axon Instruments, Molecular Devices).

### Drugs

Geneticin and ATP-sodium salt were obtained from Calbiochem (La Jolla, CA), whereas CsOH was from Aldrich Chemicals (Milan, Italy). DMEM, FCS, penicillin, streptomycin, and nonessential amino acids were from Invitrogen (San Giuliano Milanese, Italy). All the other chemicals were of analytical grade and were from Sigma (Milan, Italy).

### Data analysis

All data are reported as means  $\pm$  SE. When comparing two data sets, the Student's *t*-test for paired or unpaired data were used as appropriate whereas, repeated-measure ANOVA was used for multiple group comparison. Statistical comparisons were carried out using the Graph-PAD 2.04 software suite (GraphPad Software, San Diego, CA). Curve fitting was performed with the Sigma-plot 5.0 (SPSS) or the N-fit (The University of Texas, Medical Branch at Galveston, Galveston, TX) software.

## RESULTS

### Effect of $\text{Zn}^{2+}$ on steady-state $\text{Ca}_v3.3$ channel activation and inactivation

To study the effect of  $\text{Zn}^{2+}$  (300  $\mu\text{M}$ ) on the voltage dependence of activation, current versus voltage ( $I$ - $V$ ) curves were obtained from  $\text{Ca}_v3.3$  cells. Briefly, repetitive step depolarizations were delivered at progressively more positive voltages both in the presence and in the absence of this metal (Fig. 1A). The values of half voltage ( $V_{1/2m}$ ) and slope ( $k_m$ ) of the channel

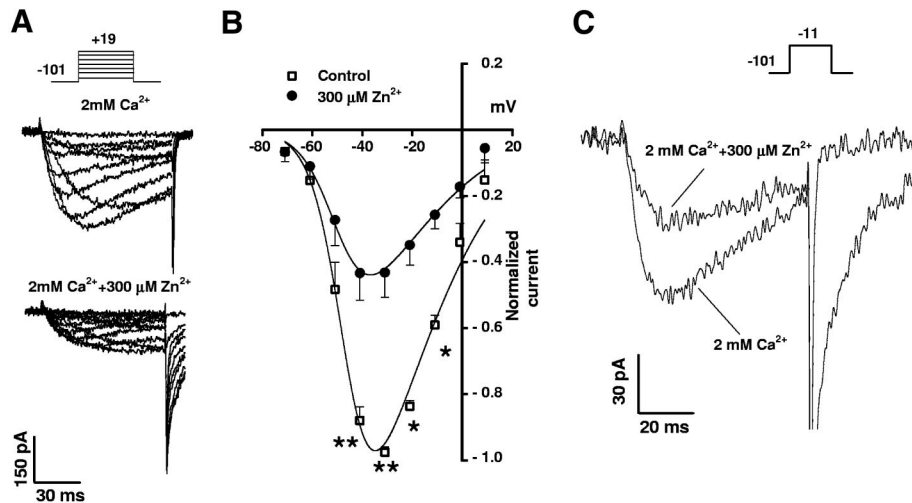


FIG. 1. Effects exerted by  $\text{Zn}^{2+}$  on voltage dependence of activation and whole cell  $\text{Ca}^{2+}$  permeability in  $\text{Ca}_v3.3$  cells. **A**: representative current traces elicited by consecutive step depolarizations (75-ms duration) to progressively more positive voltages (from  $-71$  to  $+19$  mV in increments of  $\sim 10$  mV) in a  $\text{Ca}_v3.3$  cell perfused with  $2$  mM  $\text{Ca}^{2+}$  before (top) and after (bottom) addition of  $300$   $\mu\text{M}$   $\text{Zn}^{2+}$  to the perfusion medium. **B**: mean current-to-voltage plots showing, as a function of step voltage, the means  $\pm$  SE of the maximal current amplitudes reached in 7 cells before ( $\square$ ) and after ( $\bullet$ ) the addition of  $300$   $\mu\text{M}$   $\text{Zn}^{2+}$  to the perfusion medium. —, obtained by fitting the data to the Goldman-Hodgkin current equation. \* $P < 0.05$ ; \*\* $P < 0.01$ . **C**: current traces evoked by membrane depolarization (up to  $-11$  mV, 75 ms) in a  $\text{Ca}_v3.3$  cell held at  $-101$  mV and perfused with  $2$  mM  $\text{Ca}^{2+}$  before and after  $\text{Zn}^{2+}$  addition. In this type of experiment,  $\text{Ca}_v3.3$  cells ( $n = 5$ ) were continuously perfused with  $2$  mM  $\text{Ca}^{2+}$  and 50 s after the beginning of current recordings,  $300$   $\mu\text{M}$   $\text{Zn}^{2+}$  was added to the extracellular solution. In **A** and **C**, voltage protocols are reported in the insets, where numbers indicate the voltage applied expressed in mV.

activation were extrapolated by fitting the data to the Goldman and Hodgkin current equation reported in METHODS (Fig. 1B). The values obtained with this approach were not significantly different in the two experimental groups neither in the case of  $V_{1/2m}$  ( $-48.36 \pm 0.73$  vs.  $-48.77 \pm 1.21$  mV, before and after  $\text{Zn}^{2+}$  addition, respectively) nor in the case of  $k_m$  ( $8.26 \pm 0.2$  vs.  $7.25 \pm 0.63$ , before and after  $\text{Zn}^{2+}$  addition, respectively). Curve fitting also provided an estimate of the whole cell  $\text{Ca}^{2+}$  permeability in the presence and in the absence of  $\text{Zn}^{2+}$ , thereby showing that this metal reduces cell permeability by 55.6% (from  $0.036 \pm 0.004$  to  $0.0237 \pm 0.003$   $\text{cm}^3/\text{s}$ ,  $P < 0.001$ ). This reduction is close to that of inward  $\text{Ca}^{2+}$  current measured either with the protocol shown in Fig. 1, **A** and **B** ( $56.7 \pm 7.4\%$ ) or by repetitive step depolarization up to  $-11$  mV ( $56.7 \pm 6.9\%$ ; Fig. 1C) (cf., Jeong et al. 2003). These findings suggest that even in the presence of high micromolar concentrations of  $\text{Zn}^{2+}$   $\text{Ca}_v3.3$  channel activity is not totally blocked and, therefore its presence in the extracellular solution does not hamper the flow of  $\text{Ca}^{2+}$  through  $\text{Ca}_v3.3$  channels.

To study the effect of  $\text{Zn}^{2+}$  on the voltage dependence of inactivation, 10-s prepulses of increasing voltages (from  $-121$  up to  $-11$  mV with 10-mV increments) were delivered to two different groups of  $\text{Ca}_v3.3$  cells: one perfused with  $2$  mM  $\text{Ca}^{2+}$  and the other with the same solution plus  $300$   $\mu\text{M}$   $\text{Zn}^{2+}$ ; then, after setting back membrane potential to  $-101$  mV for 5 ms, cells were step depolarized up to  $-11$  mV for 75 ms (Fig. 2A). Steady-state inactivation curves were generated by plotting the maximal amplitude of the inward currents evoked by each step, as a function of prepulse voltages (Fig. 2B). Mean half voltages ( $V_{1/2h}$ ) of inactivation obtained by fitting the data to a charge-voltage Boltzman Eq. 11 were not significantly different in the two groups of  $\text{Ca}_v3.3$  cells ( $V_{1/2h} = -79.2 \pm 2.5$  vs.  $-79.6 \pm 2.3$  mV, in  $\text{Ca}^{2+}$  and  $\text{Zn}^{2+}$  groups, respectively). Instead, slope ( $K_h$ ) values were significantly higher in the presence of  $\text{Zn}^{2+}$  ( $6.1 \pm 0.6$  vs.  $9.2 \pm 0.9$ ,  $P < 0.05$ ; Fig. 2B) in  $\text{Ca}^{2+}$  and  $\text{Zn}^{2+}$  groups, respectively.

#### Effect of $\text{Zn}^{2+}$ on $\text{Ca}_v3.3$ activation and inactivation kinetics

Accordingly to the Hodgkin and Huxley formalism (1952), channel opening and inactivation do not occur instantaneously but take time to appear. Therefore the amount of current that goes through a voltage-gated ion channel at each given time after a depolarization is determined not only by membrane voltage and by the steady-state activation and inactivation of the channels but also by the kinetics of the activation and inactivation gates, which are both intrinsically voltage dependent and can be described with appropriate activation ( $\tau_m$ ) and inactivation ( $\tau_h$ ) time constants. This strict voltage dependence of activation and inactivation kinetics is known to apply also to T-type channels as originally described by Coulter et al. (1989) in relay thalamic neurons and may have important functional implications when rapid phenomena such as action potential generation at the postsynaptic membrane of the *gluzinergic* synapse, occur. Accordingly, we determined the effect of  $\text{Zn}^{2+}$  on  $\text{Ca}_v3.3$  channel activation and inactivation gate kinetics at different membrane voltages. For values of membrane potential more positive than the threshold for  $\text{Ca}_v3.3$  channel opening, activation ( $\tau_m$ ) and inactivation ( $\tau_h$ ) time constants were determined by fitting the current traces elicited by the step depolarization protocol reported in Fig. 1 to the Hodgkin and Huxley  $m^2h$  equation described by McCormick and Huguenard (1992). Using this approach we found that  $\text{Zn}^{2+}$  significantly slowed both the activation time constant ( $\tau_m$ ) and the inactivation time constant ( $\tau_h$ ; Fig. 3A). When  $\text{Ca}_v3.3$  cells were exposed to  $100$   $\mu\text{M}$   $\text{Zn}^{2+}$  a significant slowing down of current inactivation was observed ( $\tau_h$  percent increase  $363.6 \pm 117.0\%$  of control values,  $P < 0.05$ , repeated-measure ANOVA), whereas channel activation was not affected (Fig. 3B). Conversely,  $\text{Zn}^{2+}$  was ineffective at concentrations of  $\leq 30$   $\mu\text{M}$  (Fig. 3B).

At voltages more negative than the threshold for  $\text{Ca}_v3.3$  channel opening, the values of the time constant of the activation gate

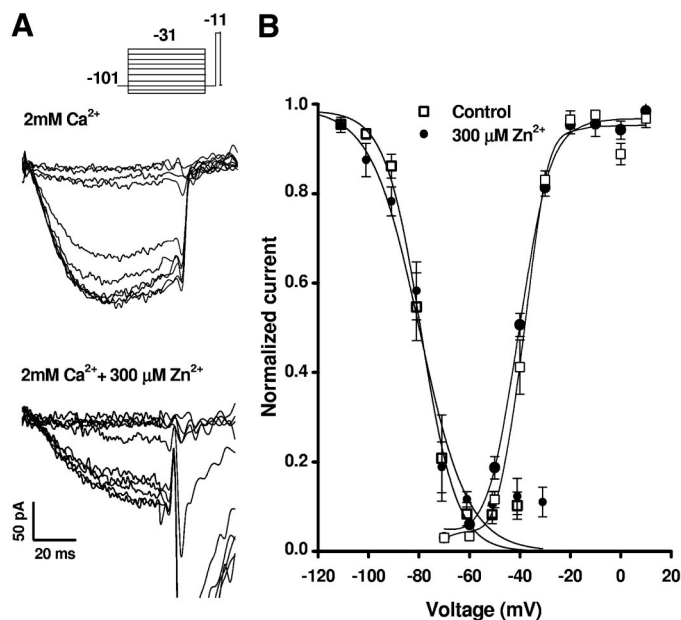


FIG. 2.  $\text{Ca}_v3.3$  current steady-state inactivation in the presence and absence of  $\text{Zn}^{2+}$ . *A*: current traces evoked by repeated membrane depolarizations up to  $-11$  mV (75-ms duration; frequency 0.07 Hz) that were delivered after a conditioning prepulse of 10-s duration in 2  $\text{Ca}_v3.3$  cells perfused with 2 mM  $\text{Ca}^{2+}$  (top) or with 2 mM  $\text{Ca}^{2+}$  + 300  $\mu\text{M}$   $\text{Zn}^{2+}$  (bottom); these cells are representative of 2 different groups each of 10 cells. The voltage protocol is reported in the inset where numbers indicate the voltage applied expressed in mV. *B*: steady-state activation and inactivation curves obtained in cells perfused with 2 mM  $\text{Ca}^{2+}$  in the absence ( $n = 10$ ) and in the presence ( $n = 10$ ) of 300  $\mu\text{M}$   $\text{Zn}^{2+}$ . Steady-state inactivation curves were drawn from the data obtained by applying the protocol shown in *A*. Each data point represents the means  $\pm$  SE of the individual values of the maximal inward current amplitude attained in all the cells of the control and  $\text{Zn}^{2+}$  groups when the plasmamembrane potential was depolarized up to 0 mV after each prepulse.  $h_\infty$  curves (—) were obtained by fitting the data to the Boltzmann's Eq. 11 as reported in METHODS.

$\tau_m$  values were obtained by measuring the decay kinetics of the tail currents that appeared when the membrane was repolarized at different voltages after a step depolarization up to  $-11$  mV (Fig. 4A). These tails relaxed with a bi-exponential kinetics characterized by fast ( $\tau_1$ ) and slow ( $\tau_2$ ) deactivation kinetic con-

stants. By comparing the tail current  $\tau$  values in the presence and in the absence of 300  $\mu\text{M}$   $\text{Zn}^{2+}$ , we found that this metal slowed down the deactivation kinetics at all the tested voltages in the interval between  $-141$  and  $-71$  mV (Fig. 4, *B* and *C*). It is worth noticing that in the range of the voltages around  $-70$  mV, i.e., close to resting potential in nRT neurons,  $\tau_1$  values were similar in the presence and in the absence of  $\text{Zn}^{2+}$ . Importantly,  $\text{Zn}^{2+}$  effect on deactivation kinetics was also observed when  $\text{Ca}_v3.3$  cells were exposed to a concentration of 100  $\mu\text{M}$  of this metal ( $\tau_2$  percent increase  $568.7 \pm 140.4\%$  of control values,  $P < 0.05$ ) but not when concentrations of  $\leq 30$   $\mu\text{M}$  were used (Fig. 3B).

At voltages more negative than the threshold for  $\text{Ca}_v3.3$  channel opening, the values of the time constant of the inactivation gate ( $\tau_h$ ) were obtained by measuring the kinetics at which  $\text{Ca}_v3.3$  channels recovered from inactivation. To this aim,  $\text{Ca}_v3.3$  channels were first inactivated by applying a 10-s inactivating prepulse to  $-51$  mV. Then the membrane was repolarized and step depolarizations up to  $-11$  mV were delivered at progressively longer time intervals from the end of the prepulse (Fig. 5A). The repolarization voltage was set at different values (from  $-111$  to  $-71$  mV) in different groups of cells. Using this approach, we found that  $\text{Zn}^{2+}$  caused a significant slowing of recovery from inactivation when the repolarization voltage was set at  $-71$  mV (Fig. 5B).

A bell-shaped voltage-dependence curve similar to what described by Hodgkin and Huxley (1952) for  $\text{Na}^+$  and  $\text{K}^+$  currents and by McCormick and Huguenard (1992) for native T-type currents was obtained when the values of the time constant of the activation gate  $\tau_m$  values, plotted as a function of voltage, were fitted to the Eq. 12 reported in METHODS. The curve obtained by plotting the  $\tau_m$  values in the presence of 300  $\mu\text{M}$   $\text{Zn}^{2+}$  was significantly larger at all the voltages tested in the range between  $-131$  and  $-1$  mV, reflecting both the slowing of channel activation at suprathreshold voltages and the slowing of channel deactivation at subthreshold voltages (Fig. 6A). Similarly, a bell-shaped curve was generated when the values of the time constant of the inactivation gate  $\tau_h$  data were plotted as a function of the voltage and fitted to the equation 12 reported in METHODS (Fig. 6B). In the voltage range

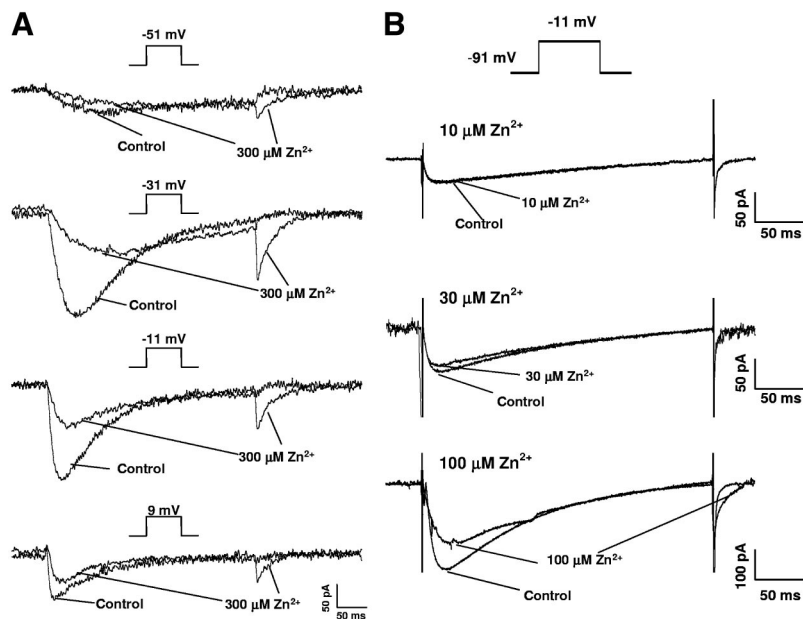


FIG. 3. Effect of different  $\text{Zn}^{2+}$  concentrations on  $\text{Ca}_v3.3$  current kinetics. *A*: slowing of  $\text{Ca}_v3.3$  current kinetics on exposure to 300  $\mu\text{M}$   $\text{Zn}^{2+}$ . Current traces were recorded in the same  $\text{Ca}_v3.3$  cell in response to consecutive step depolarizations delivered at progressively more positive voltages. Cells were held at  $-90$  mV, and step voltage was increased in 10-mV increments with an interepisode interval of 10 s. Long depolarizations (300 ms) were applied to resolve the slow inactivation of current traces at the more negative voltages. *B*: current traces recorded in three different  $\text{Ca}_v3.3$  cells before and after the addition to the extracellular solution of 10, 30, and 100  $\mu\text{M}$   $\text{Zn}^{2+}$  (from the top to the bottom). Cells were held at  $-91$  mV and step depolarized up to  $-11$  mV. Long depolarizations (300 ms) were applied to resolve the slow inactivation of current traces at the more negative voltages. Each trace is from a different cell representative of a group of 5. In *A* and *B*, voltage protocols are reported in the insets, where numbers indicate the voltage applied expressed in mV.

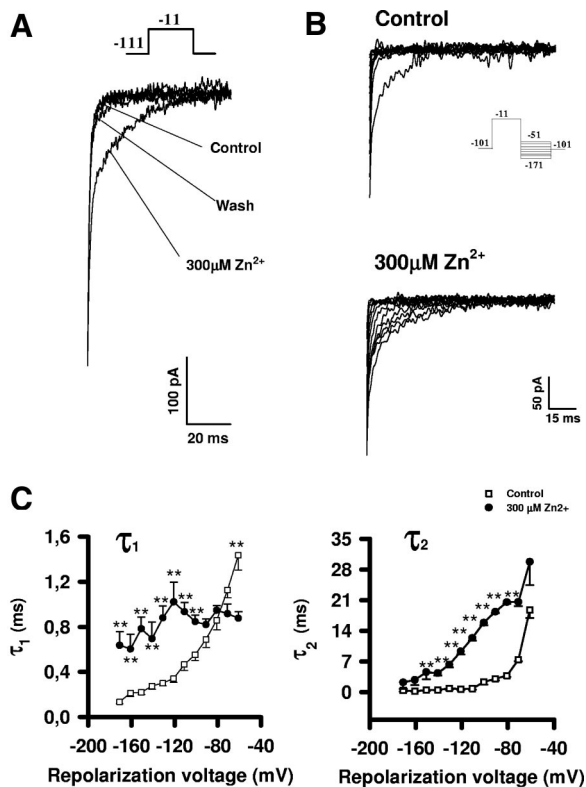


FIG. 4.  $\text{Ca}_v3.3$  current deactivation in the presence and in the absence of  $\text{Zn}^{2+}$ . *A*: tail current traces evoked by membrane repolarization in 2 different cells, one perfused with 2 mM  $\text{Ca}^{2+}$  without  $\text{Zn}^{2+}$  and the other with 2 mM  $\text{Ca}^{2+}$  plus 300  $\mu\text{M}$   $\text{Zn}^{2+}$ . Tail currents were evoked by membrane repolarization at  $-111$  mV as indicated in the *inset*. *B*: tail current traces evoked by membrane repolarization at different voltages in 2  $\text{Ca}_v3.3$  cells exposed to 2 mM  $\text{Ca}^{2+}$  with or without 300  $\mu\text{M}$   $\text{Zn}^{2+}$ . For sake of clarity, only the tails are shown in *A* and *B*. *C*: mean  $\tau_1$  (*left*) and  $\tau_2$  (*right*) values as a function of the repolarization voltage obtained by the biexponential fitting of tail current decay. Each data point is the means  $\pm$  SE of the values calculated by the biexponential fitting of the current traces recorded at each  $\text{Zn}^{2+}$  concentration in 6 cells. \* $P < 0.05$ ; \*\* $P < 0.01$ .

between  $-91$  and  $-41$  mV, the curve obtained in the presence of 300  $\mu\text{M}$   $\text{Zn}^{2+}$  was significantly larger than in control, reflecting the slowing effect of this ion on recovery from inactivation at subthreshold voltages and on current inactivation at suprathreshold voltages.

#### Effects of $\text{Zn}^{2+}$ on the currents evoked by mock action potentials in $\text{Ca}_v3.3$ cells

To explore how  $\text{Zn}^{2+}$ -induced modifications in  $\text{Ca}_v3.3$  channel gating could affect the ability of  $\text{Ca}_v3.3$  channels to generate action potentials, we measured the  $\text{Ca}^{2+}$  currents elicited by mock action potentials delivered to  $\text{Ca}_v3.3$  cells through the patch pipette (Kozlov et al. 2005). Cells were first depolarized by delivering an ascending ramp from  $-101$  up to  $+39$  mV in 3 ms and, then, immediately repolarized by a second descending ramp bringing the potentials down to  $-101$  mV in 6 ms. This protocol elicited large inward currents in cells perfused with 2 mM  $\text{Ca}^{2+}$  (Fig. 7). When the same cells were perfused with 2 mM  $\text{Ca}^{2+}$  + 300  $\mu\text{M}$   $\text{Zn}^{2+}$ , the currents were significantly smaller, peaked significantly later, and persisted for a significantly longer period of time because their

relaxation kinetics was slowed (Fig. 7). These data indicate that, in the presence of  $\text{Zn}^{2+}$ ,  $\text{Ca}^{2+}$  influx through  $\text{Ca}_v3.3$  channels is maintained for a significantly longer time interval than under control condition, thus suggesting that  $\text{Zn}^{2+}$  can influence excitability in cells expressing  $\text{Ca}_v3.3$  channels.

#### $\text{Zn}^{2+}$ effects on the frequency and duration of action potentials in simulated nRT cells

To establish whether  $\text{Zn}^{2+}$  modifies the frequency and/or the duration of neuronal action potential trains, we inserted  $\text{Zn}^{2+}$ -induced changes in  $\text{Ca}_v3.3$  channel gating parameters into the NEURON simulated model developed by Destexhe et al. (1996). This model reproduces the electrophysiological behavior of nRT neurons, a cell type where T-type channels participate in depolarization-induced action potentials and are required for triggering rebound burst firing. To run the nRT simulation, we introduced the kinetic parameters obtained from  $\text{Ca}_v3.3$  cells exposed or not to  $\text{Zn}^{2+}$  into the IT2 model file, which provides to the NEURON program the parameters needed to build up the simulated T-type current (see METHODS). Conversely, the parameters describing the contribution of the other ion channels, i.e., voltage-gated  $\text{Na}^+$  and  $\text{K}^+$  channels, included in the NEURON model were not modified.

When the injection of a 200-ms hyperpolarizing current (0.3 nA) pulse was simulated, we observed under control conditions the appearance of a burst firing with the crescendo-decrescendo pattern typical of nRT cells; in contrast, this protocol was characterized by a dramatic increase in burst firing frequency in the presence of  $\text{Zn}^{2+}$  (Fig. 8A). It is worth noticing that the burst firing onset in the presence of  $\text{Zn}^{2+}$  was significantly delayed and that the simulated neuron returned to baseline condition in  $\sim 300$  ms from the beginning of burst firing. Similarly, when we simulated the injection of a 200-ms depolarizing current (0.3 nA) pulse, we observed an increase in action potential frequency in the presence of  $\text{Zn}^{2+}$  (Fig. 8B). To reproduce the  $\text{Zn}^{2+}$ -induced blockade of  $\text{Ca}_v3.3$  channels, both the simulation involving the injection of a negative current pulse and that involving the injection of a positive current pulse were run introducing into the model a value for  $\text{Ca}^{2+}$  whole cell conductance 55.5% lower than that used in control cell recording. Therefore these data suggest that, despite the reduction in the amplitude of the currents flowing through  $\text{Ca}_v3.3$  channels by  $\text{Zn}^{2+}$ , this metal caused a substantial increase in neuronal excitability.

#### Effects of $\text{Zn}^{2+}$ chelation on spontaneous epileptiform activity in thalamocortical slices

Overall, the data obtained in vitro from HEK  $\text{Ca}_v3.3$  cells and from the nRT computer model indicate that  $\text{Zn}^{2+}$  may exert an excitatory effect on thalamic activity. To further test this hypothesis, we explored the consequences of  $\text{Zn}^{2+}$  chelation in an acute thalamocortical slice preparation. Spontaneous field activity was induced by perfusing these slices with 50  $\mu\text{M}$  4AP (Biagini et al. 2001). As illustrated in Fig. 9A (control panel), two different types of epileptiform field activity were observed: prolonged ( $>8$  s) ictal-like discharges and short (0.5–4 s) interictal-like events. As expected with preserved thalamocortical connectivity, the majority of discharges occurred synchronously in the cortex, VB and nRT, with a few

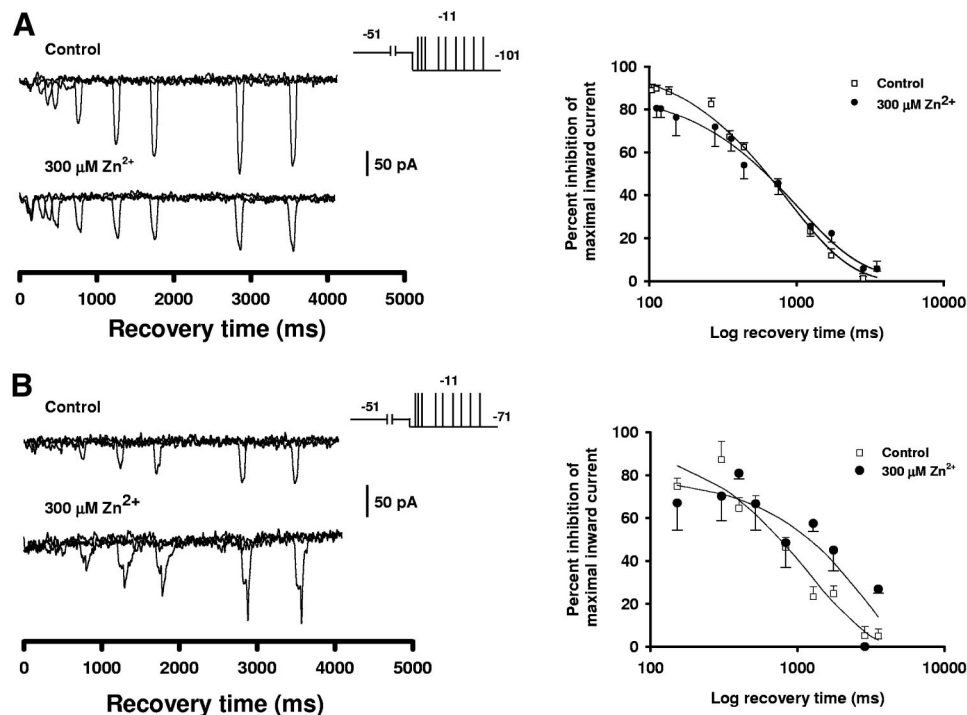


FIG. 5.  $\text{Ca}_v3.3$  current recovery from inactivation in the presence and absence of  $\text{Zn}^{2+}$ . *Left*: families of current traces elicited by repeated 80-ms step depolarizations up to  $-11$  mV, delivered at progressively longer time intervals after repolarizing the plasma-membrane to  $-101$  (A) or  $-71$  (B) mV after a 10-s inactivating prepulse to  $-51$  mV. Both in A and B, 2 different  $\text{Ca}_v3.3$  cells, one perfused with 2 mM  $\text{Ca}^{2+}$  (top) and the other with 2 mM  $\text{Ca}^{2+}$  plus 300  $\mu\text{M}$   $\text{Zn}^{2+}$  (bottom), are shown. *Right*: mean recovery from inactivation curves obtained by averaging the data obtained in  $\text{Ca}_v3.3$  cells repolarized to  $-101$  mV (A) or  $-71$  mV (B) perfused with 2 mM  $\text{Ca}^{2+}$  in the presence and in the absence of 300  $\mu\text{M}$   $\text{Zn}^{2+}$ . Each data point represents the means  $\pm$  SE of all the maximal amplitude of the currents elicited after the inactivating prepulse in each cell under control and  $\text{Zn}^{2+}$  at the time indicated in the graph, expressed as percentages of the maximal inward current recorded during the entire protocol, which was conventionally set as the 100%. The cells depicted in A (*right*) are representative of a group of 9 (2 mM  $\text{Ca}^{2+}$  group) and of 11 cells ( $\text{Zn}^{2+}$  group), whereas the cells depicted in B (*right*) are representative of a group of 4 cells both in the case of the control and of the  $\text{Zn}^{2+}$  exposed cells. In A and B, voltage protocols are reported in the insets where numbers indicate the voltage applied expressed in mV.

tens of ms delay between these structures (cf., Biagini et al. 2001). After a 15- to 30-min exposure to the  $\text{Zn}^{2+}$  chelator TPEN (300  $\mu\text{M}$ ), ictal discharges significantly decreased in frequency (Fig. 9A, TPEN panel) in all structures while interictal discharges remain unchanged. These data are summarized in Fig. 9, B and C. It should be emphasized that TPEN did not induce any significant change in the mean amplitude and duration of either ictal or interictal discharges and that TPEN-induced effect on ictal discharge occurrence was not reversible on drug washout.

## DISCUSSION

The present paper demonstrates that high micromolar concentrations of  $\text{Zn}^{2+}$  slow down the gating kinetics of  $\text{Ca}_v3.3$  channels while only partially reducing their  $\text{Ca}^{2+}$  permeability. We also provide evidence that  $\text{Zn}^{2+}$  induces an increase in the frequency of  $\text{Ca}_v3.3$ -dependent burst firing as indicated by incorporating the  $\text{Zn}^{2+}$ -induced changes in gating kinetics into computer simulations of nRT neuron activity. Finally, this study shows that chelation of endogenous  $\text{Zn}^{2+}$  reduces the occurrence of ictal-like epileptiform events in thalamocortical slices maintained *in vitro*. Although it is well established that  $\text{Zn}^{2+}$  can influence the gating properties of several voltage-gated ion channels (Harrison and Gibbons 1994; Mathie et al. 2006), this is the first report to explore the effect of  $\text{Zn}^{2+}$  on T-type channel-dependent firing in simulated nRT neurons and the first to establish a role for endogenous  $\text{Zn}^{2+}$  in the activity of the thalamocortical system.

Surface charge screening by  $\text{Zn}^{2+}$  represents an obvious possible explanation for the effects induced by this ion on channel gating. In line with this view, it has been reported that like other metal ions,  $\text{Zn}^{2+}$  effectively binds to and neutralizes negative surface charges on the membrane, thus modifying the local electrical field around ion channels (Hille 1992). Even though the shielding effect of high concentrations of  $\text{Zn}^{2+}$  may have major consequences on channel gating, this mechanism does appear to be relevant when  $\text{Ca}_v3.3$  cells were exposed to 300  $\mu\text{M}$   $\text{Zn}^{2+}$ . In fact, while the Gouy-Chapman theory (Hille 1992) predicts that the half voltages for channel activation and inactivation and the  $\tau_m$  and  $\tau_h$  curves would be shifted rightward owing to surface charge screening, we did not find any significant shift suggesting that the concentration used in this study (i.e., 300  $\mu\text{M}$ ) was too low to significantly shield surface charges. Interestingly, it has been proposed that metal ions, such as  $\text{Ni}^{2+}$  or  $\text{La}^{3+}$ —which are known to bind to ion channels—affect channel gating in a way that cannot be explained merely on the basis of the Gouy-Chapman theory of surface screening (Armstrong and Cota 1990; Elinder et al. 1996; Hille 1992). This could also be the case of  $\text{Zn}^{2+}$  that binds to the channel pore of voltage-dependent  $\text{Ca}^{2+}$  channels. In this context, it is tempting to speculate that  $\text{Zn}^{2+}$ , while standing into the pore of  $\text{Ca}_v3.3$  channels, may cause structural rearrangements of this channel region that contribute to the gating process. In line with this view, a crucial role in the gating process has been demonstrated for the pore region of T-type channels, the gating of which has been shown to be

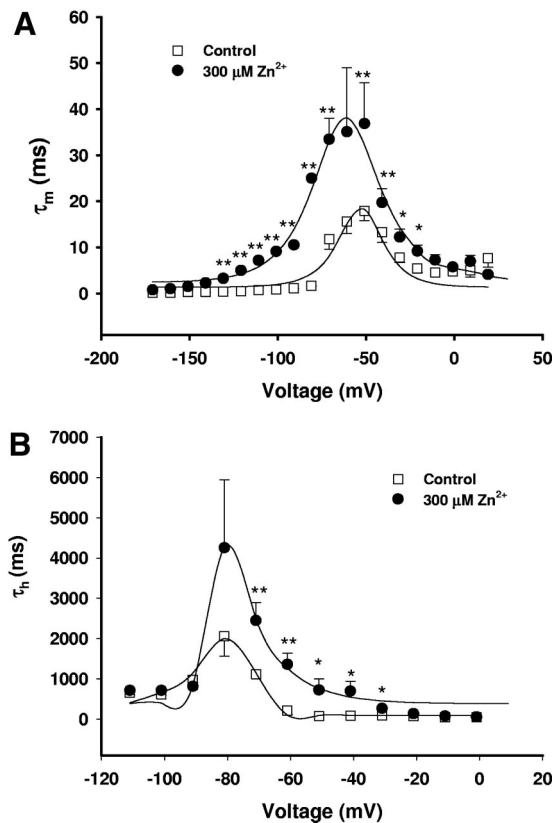


FIG. 6. Voltage-dependence curves of the activation and inactivation time constants of  $\text{Ca}_v3.3$  channels in the presence and in the absence of  $\text{Zn}^{2+}$ . A: voltage-dependence curve of the time constant of the activation gate. For voltages more negative than  $-61$  mV, each data point represents the means  $\pm$  SE of the values of weighted deactivation  $\tau$  obtained by applying the protocol described in Fig. 5A at the corresponding repolarization voltage. For voltages equal to or more positive than  $-61$  mV, the data points represent the values of  $\tau$  obtained by fitting the current traces elicited by the step protocol reported in Fig. 1A to Eq. 5. B: voltage-dependence curve of the time constant of the inactivation gate. For voltages more negative than  $-61$  mV, each data point represents the means  $\pm$  SE of the time constants of recovery from inactivation obtained by applying the protocol described in Fig. 4A at the corresponding repolarization voltage. For voltages equal to or more positive than  $-61$  mV, the data points represent the values of the time constants of inactivation obtained by fitting to Eq. 5 the current traces elicited by step depolarization according to the protocol reported in Fig. 1A. Both in A and in B, —, obtained by fitting the data to Eq. 12. \* $P < 0.05$ ; \*\* $P < 0.01$ .

influenced by changes in the nature of the permeant ion (Shuba et al. 1991) or by point mutations in the selectivity filter of the channel pore (Talavera et al. 2003).

As the presence of  $\text{Zn}^{2+}$  dramatically slowed down  $\text{Ca}_v3.3$  channel inactivation and deactivation kinetics, we believe that exposure of  $\text{Ca}_v3.3$  to  $\text{Zn}^{2+}$  alters the function of this class of T-type channels during physiological processes that are characterized by rapid changes in membrane voltage. This is the case, for instance, of action potential generation and propagation. Therefore we hypothesize that  $\text{Zn}^{2+}$  would modify the response of  $\text{Ca}_v3.3$  channels to incoming action potentials and/or their ability to generate hyperpolarization-induced low-threshold spikes, which entrain  $\text{Na}^+$ -dependent action potential bursts (Perez-Reyes 2003). Our data presented support this idea. Indeed by exploring the ability of  $\text{Ca}_v3.3$  channels to open in response to mock action potential, we found that the shape of  $\text{Ca}^{2+}$  currents was significantly different during  $\text{Zn}^{2+}$  application. Thus in the presence of this ion, the currents

elicited by mock action potential were smaller but more persistent than under control conditions, suggesting that when  $\text{Zn}^{2+}$  is released in the extracellular compartment,  $\text{Ca}^{2+}$  influx through T-type channels lasts longer than under control conditions. Accordingly, using the NEURON computer simulation of nRT neurons (Dexthex et al. 1996; Murbartian et al. 2004), we found that  $\text{Zn}^{2+}$  increases the frequency of burst firing. This type of computer simulation has already been adapted to  $\text{Ca}_v3.3$  cells (Murbartian et al. 2004), and simulations in HEK-293 cells have been used to infer conclusions on neuronal T-type channel activity in physiological (Kozlov et al. 1999) and pathophysiological conditions (Vitko et al. 2005).

Assuming that our simulation data can be extrapolated to real nRT cells, the ability of  $\text{Zn}^{2+}$  to affect  $\text{Ca}_v3.3$ -dependent burst firing may have relevant implications in pathophysiological conditions in which the extracellular concentration of  $\text{Zn}^{2+}$  released from the terminals of the glutamergic fibers, which impinge onto nRT neurons (Mengual et al. 2001), reaches values close to what used in our experiments (300  $\mu\text{M}$ ). The extracellular concentrations of  $\text{Zn}^{2+}$  have not been clearly established to date (Frederickson et al. 2006a; Kay 2003). It is, however, believed that  $\text{Zn}^{2+}$  release is negligible under basal conditions (Frederickson et al. 2006b), whereas it can increase up to 30–100  $\mu\text{M}$  during ischemia or seizures (Thompson et al. 2002; Ueno et al. 2002). In addition, much higher concentrations of this ion are presumably reached in restricted areas around the site of release of  $\text{Zn}^{2+}$ -containing vesicles. It should be emphasized that we observed relevant kinetic effects also in cells exposed to 100  $\mu\text{M}$   $\text{Zn}^{2+}$ . In addition, it should also be noticed that, concomitantly with intense synaptic stimulation, as in epilepsy (Heinemann and Louvel 1983; Heinemann et al. 1977) or ischemia (Harris et al. 1981), extracellular  $\text{Ca}^{2+}$  concentration is expected to drop as a consequence of neuronal sink action. This could significantly shift rightward the  $\text{Zn}^{2+}$  effect-concentration curve assuming a binding competition between  $\text{Ca}^{2+}$  and  $\text{Zn}^{2+}$  as should happen if, as we hypothesized, the pore of  $\text{Ca}_v3.3$  could represent the site for  $\text{Zn}^{2+}$  action on  $\text{Ca}_v3.3$  channel kinetics.

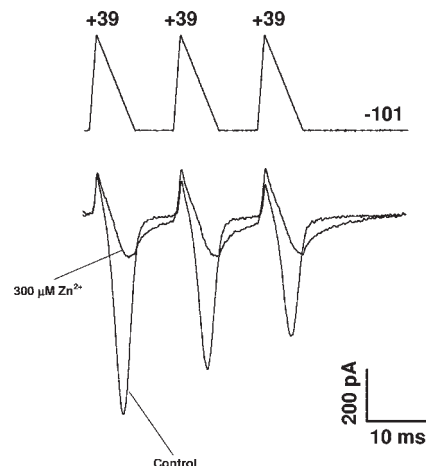


FIG. 7.  $\text{Ca}^{2+}$  currents evoked by mock action potentials in the presence and in the absence of  $\text{Zn}^{2+}$ . Current traces elicited by a train of 3 mock action potentials generated by the patch amplifier according to the protocol reported in the inset where the numbers indicate the applied voltage expressed in mV. The traces shown were obtained from a single  $\text{Ca}_v3.3$  cell representative of a group of 7 before and after the addition of  $\text{Zn}^{2+}$  (300  $\mu\text{M}$ ) to the bathing 2 mM  $\text{Ca}^{2+}$  solution.

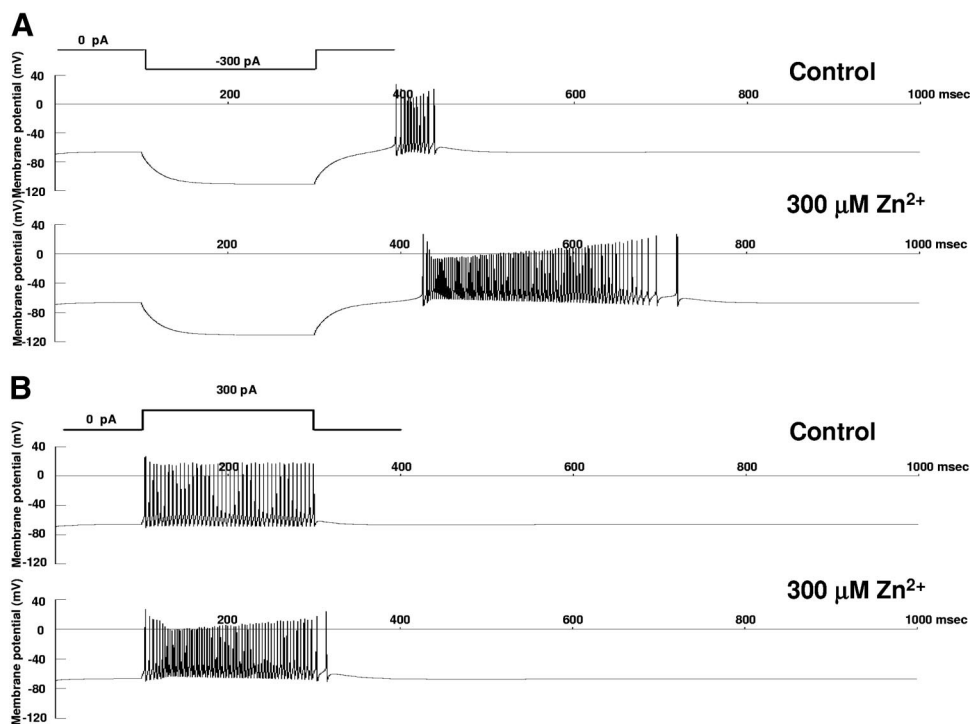


FIG. 8. Computer simulation of  $Ca_v3.3$ -dependent nRT burst firing in the presence and in the absence of  $Zn^{2+}$ . *A*: burst firing elicited by the injection of a pulse of hyperpolarizing current ( $-0.3$  nA) in the absence (*top*) and in the presence (*bottom*) of  $300 \mu M Zn^{2+}$  using the NEURON nucleus reticularis thalami (nRT) cell model simulation as detailed in METHODS. *B*: trains of simulated action potentials elicited by the injection of a 200-ms depolarizing current pulse ( $0.3$  nA) in the absence (*top*) and in the presence (*bottom*) of  $300 \mu M Zn^{2+}$  in the same model nRT cell as in *A*. Both in *A* and in *B*, voltage traces were generated using the option "burst behavior in a 3-compartment model" of the NEURON software with the resting potential set at  $-70$  mV and the gating kinetic constants obtained by applying the experimental protocols reported in Figs. 1–6 and described throughout the text. For more details, see METHODS.

On the basis of these considerations, we believe that our data have implications in brain ischemia or in epilepsy, two neurological conditions in which extracellular  $Zn^{2+}$  concentrations reach high micromolar values. This hypothesis is supported by the results obtained from acute thalamocortical slices exposed to the convulsant drug 4AP, which represents an in vitro model of epileptic discharge (Biagini et al. 2002; D'Arcangelo et al. 2002). We found that exposure to the  $Zn^{2+}$  chelator TPEN decreased the occurrence of 4AP-induced ictal-like discharges in nRT and cortex. TPEN presumably chelated the intracellular releasable  $Zn^{2+}$  as suggested by the ability of this drug to deplete brain terminals from  $Zn^{2+}$  (Cuajungco and Lees 1996). Despite its ability to chelate also iron and copper TPEN is usually

considered a selective  $Zn^{2+}$  chelator, and it has been used to assess the role of this ion in neurotransmission in the hippocampus (Matias et al. 2006).

The ability of exogenous  $Zn^{2+}$  to increase the frequency of thalamocortical discharges in brain slices has been reported by Gibbs et al. (2000). However, no information is available on the physiological meaning of this  $Zn^{2+}$  action in the thalamocortical system; in addition, it was unknown whether endogenous  $Zn^{2+}$  could exert similar effects. At the best of our knowledge, our data represent the first evidence in favor of the idea that endogenous  $Zn^{2+}$  plays a role in thalamocortical excitability as shown by the dramatic consequences of its chelation. This raises the question of what are the sources of the endogenous  $Zn^{2+}$  affecting thalamocortical discharges.

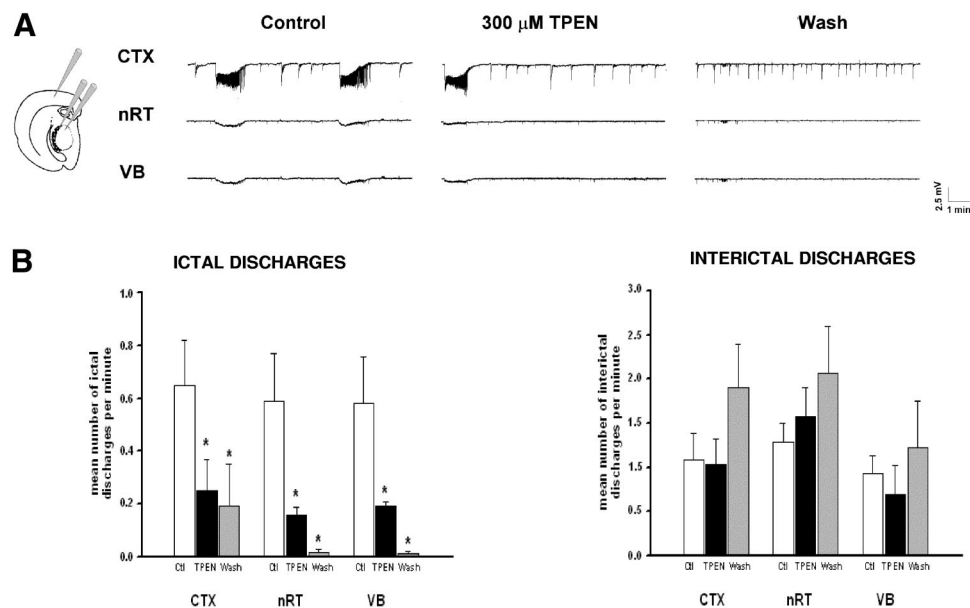


FIG. 9. Effects of  $Zn^{2+}$  chelation on spontaneous epileptiform discharges induced by 4-aminopyridine in acute thalamocortical slices. *A*: extracellular field potentials recorded before, during and after exposure to the  $Zn^{2+}$  chelator *N,N,N',N'*-tetrakis(2-pyridylmethyl) ethylenediamine (TPEN,  $300 \mu M$ ). The recording electrodes were positioned in the parietal cortex (CTX) in the more dorsal portion of nRT and ventrobasal nucleus (VB) as illustrated in the inset. *B*: effects induced by TPEN on the frequency of ictal and interictal discharges in 5 thalamocortical slices. \**P* value  $< 0.05$  as evaluated with repeated-measure ANOVA followed by the Neuman-Keuls test.

The rat cortex is rich in Zn<sup>2+</sup>, which mostly originates into the cortex itself as cortico-cortical connections are enriched in synaptic Zn<sup>2+</sup> (Casanovas-Aguilar et al. 1998, 2002). In contrast, projecting thalamocortical fibers connecting the VB with cortex are not zincergic (Brown and Dyck 2005). However, dense zincergic terminals are concentrated in specific thalamic regions such as the dorsal portion of nRT, where we positioned our recording electrode; in addition, both anterodorsal and lateral dorsal thalamic nuclei display intense Timm staining (Mengual et al. 2002). Finally, zincergic terminals into the thalamus appear to have a cortical origin, thus identifying the zincergic thalamic afferents as a subset of glutamatergic corticothalamic fibers. As the ventrobasal thalamus is not significantly innervated by zincergic fibers and exogenous Zn<sup>2+</sup> does suppress the activity of thalamic relay neurons (Noh and Chung 2003), it is unlikely that the decrease in VB ictal firing induced by Zn<sup>2+</sup> chelation could have been determined by a direct effect on thalamic relay neurons. Conversely, the most likely explanation for TPEN effect is a decrease in the excitatory drive by afferent fibers of nRT and/or cortical origin. In line with this hypothesis comes a study, which was published while the present paper was under review, showing that Zn<sup>2+</sup> does affect the gating of the nRT-specific T-type channel isoform Ca<sub>v</sub>3.3 but not that of the T-type channel isoform Ca<sub>v</sub>3.1 that is preferentially expressed in thalamic relay neurons (Traboulsie et al. 2007).

A limitation of our study is that we did not include in our computer simulation the effect of Zn<sup>2+</sup> on other ion channels such as voltage-gated Na<sup>+</sup>, I<sub>h</sub>, and type A K<sup>+</sup> channels or ligand-gated GABA<sub>A</sub> channels, which are expressed in nRT neurons and have a role in determining their electrical properties (Abbass 2006; Destexhe and Sejnowski 2003; Yue and Huguenard 2001). Evidence reported in the literature suggests that some of these mechanisms could cooperate in a determining the pro-excitatory effect of this metal ion. For instance, it has been reported that Zn<sup>2+</sup> is ineffective on voltage-gated Na<sup>+</sup> channels or induce only a marginal decrease in Na<sup>+</sup> currents (Harrison and Gibbons 1994; Horning and Trombley 2001), whereas the effect on type A K<sup>+</sup> channels is strictly voltage dependent as these currents are enhanced by Zn<sup>2+</sup> at membrane potentials more positive than -50 mV and inhibited at more negative potentials, such as those applied by us in the simulation experiments (Horning and Trombley 2001). As far as I<sub>h</sub> channels are concerned, very few data are available on Zn<sup>2+</sup> effect on these channel type, which is inhibited only by millimolar Zn<sup>2+</sup> concentrations in neuroendocrine cells (Raymond and Lapied 1999). Finally, GABA<sub>A</sub> receptor blockade in the nRT has been reported to contribute to the pro-excitatory action of exogenous Zn<sup>2+</sup> (Gibbs et al. 2000). However, it is unlikely that this can be the only factor because we have found that exogenously added Zn<sup>2+</sup> increases the frequency of thalamocortical epileptiform discharges in the presence of saturating concentrations of the GABA<sub>A</sub> receptor antagonist picrotoxin (Cataldi and Avoli, unpublished data).

In conclusion, endogenous Zn<sup>2+</sup> controls thalamocortical firing, and this effect can be at least in part determined by its ability to slow down the gating of Ca<sub>v</sub>3.3 channels, the major T-type channel isoform expressed in nRT neurons.

#### ACKNOWLEDGMENTS

The authors are indebted to Dr. E. Perez-Reyes for kindly providing the stably transfected HEK-293, to Dr. G. Panuccio for friendly help, to V. Grillo and C. Capitale for technical support, and to Dr. P. Merolla for editorial help.

#### GRANTS

This study was supported by the following grants: Programma Speciale art. 12bis comma 6, D. Lgs. 229/99, Special Project "Alzheimer 2001/2004" to L. Annunziato from the Italian Ministry of Health and Regione Campania; COFIN 2004 to M. Cataldi and L. Annunziato from the Italian Ministry of Education, University and Research; PNR-FIRBRBNE01E7YX\_007 2001 to L. Annunziato from the Italian Ministry of Education, University and Research; Ricerca Finalizzata, legge 502/92 "Geni di vulnerabilità e di riparazione DNA" to L. Annunziato from the Italian Ministry of Health; Legge regionale 28/5/02, Finanziamento 2003 to L. Annunziato from Regione Campania; Programma Operativo Regionale (POR), Centro regionale di competenza GEAR to L. Annunziato from Regione Campania; 12th Italian-Chinese Executive program for scientific and technological Cooperation for the period 2006–2009 to L. Annunziato from the Italian Foreign Ministry; the CIHR (MOP 8109) and the Savoy Foundation to M. Avoli. V. Lariccia was supported by a fellowship from the Centro Regionale di Competenza di Genomica Funzionale. M. Cataldi was supported by a travel grant from the Federico II University of Naples, "Programma di scambi internazionali con università ed istituti di ricerca stranieri per la mobilità di breve durata di docenti, ricercatori e studiosi."

#### REFERENCES

- Abbas SY, Ying SW, Goldstein PA. Compartmental distribution of hyperpolarization-activated cyclic-nucleotide-gated channel 2 and hyperpolarization-activated cyclic-nucleotide-gated channel 4 in thalamic reticular and thalamocortical relay neurons. *Neuroscience* 141: 1811–1825, 2006.
- Agmon A, Connors BW. Thalamocortical responses of mouse somatosensory (barrel) cortex in vitro. *Neuroscience* 41: 365–379, 1991.
- Armstrong CM, Cota G. Modification of sodium channel gating by lanthanum. Some effects that cannot be explained by surface charge theory. *J Gen Physiol* 96: 1129–1140, 1990.
- Biagini G, D'Antuono M, Tancredi V, Motalli R, Louvel J, D'Arcangelo G, Pumain R, Warren RA, Avoli M. Thalamocortical connectivity in a rat brain slice preparation: participation of the ventrobasal complex to synchronous activities. *Thalamus Related Syst* 310: 169–179, 2001.
- Brown CE, Dyck RH. Retrograde tracing of the subset of afferent connections in mouse barrel cortex provided by zincergic neurons. *J Comp Neurol* 486: 48–60, 2005.
- Carbone E, Lux HD. A low voltage-activated, fully inactivating Ca<sup>2+</sup> channel in vertebrate sensory neurons. *Nature* 310: 501–502, 1984.
- Casanovas-Aguilar C, Miro-Bernie N, Perez-Clausell J. Zinc-rich neurons in the rat visual cortex give rise to two laminar segregated systems of connections. *Neuroscience* 110: 445–458, 2002.
- Casanovas-Aguilar C, Reblet C, Pérez-Clausell J, Bueno-López JL. Zinc-rich afferents to the rat neocortex: projections to the visual cortex traced with intracerebral selenite injections. *J Chem Neuroanat* 15: 97–109, 1998.
- Cataldi M, Gaudio A, Lariccia V, Russo M, Amoroso S, di Renzo G, Annunziato L. Imatinib-mesylate blocks recombinant T-type calcium channels expressed in human embryonic kidney-293 cells by a protein tyrosine kinase-independent mechanism. *J Pharmacol Exp Ther* 309: 208–215, 2004.
- Cataldi M, Perez-Reyes E, Tsien RW. Differences in apparent pore sizes of low- and high-voltage-activated Ca<sup>2+</sup> channels. *J Biol Chem* 277: 45969–45976, 2002.
- Coulter DA, Huguenard JR, Prince DA. Calcium currents in rat thalamocortical relay neurons: kinetic properties of the transient, low-threshold current. *J Physiol* 414: 587–604, 1989.
- Cribbs LL, Lee JH, Yang J, Satin J, Zhang Y, Daud A, Barclay J, Williamson MP, Fox M, Rees M, Perez-Reyes E. Cloning and characterization of alpha1H from human heart, a member of the T-type Ca<sup>2+</sup> channel gene family. *Circ Res* 83: 103–109, 1998.
- Cuajungco MP, Lees GJ. Prevention of zinc neurotoxicity in vivo by N,N,N',N'-tetrakis (2-pyridylmethyl) ethylene-diamine (TPEN). *Neuroreport* 7: 1301–1304, 1996.
- D'Arcangelo G, D'Antuono M, Biagini G, Warren R, Tancredi V, Avoli M. Thalamocortical oscillations in a genetic model of absence seizures. *Eur J Neurosci* 16: 2383–2393, 2002.
- Destexhe A, Contreras D, Steriade M, Sejnowski TJ, Huguenard JR. In vivo, in vitro, and computational analysis of dendritic calcium currents in thalamic reticular neurons. *J Neurosci* 16: 169–185, 1996.

- Destexhe A, Sejnowski TJ.** Interactions between membrane conductances underlying thalamocortical slow-wave oscillations. *J Physiol Rev* 83: 1401–1453, 2003.
- Elinder F, Madeja M, Arhem P.** Surface charges of K channels. Effects of strontium on five cloned channels expressed in *Xenopus* oocytes. *J Gen Physiol* 108: 325–332, 1996.
- Fox AP, Nowycky MC, Tsien RW.** Single-channel recordings of three types of calcium channels in chick sensory neurones. *J Physiol* 394: 173–200, 1987.
- Frederickson CJ, Giblin LJ 3rd, Rengarajan B, Masalha R, Frederickson CJ, Zeng Y, Lopez EV, Koh JY, Chorin U, Besser L, Hershinkel M, Li Y, Thompson RB, Krezel A.** Synaptic release of zinc from brain slices: factors governing release, imaging, and accurate calculation of concentration. *J Neurosci Methods* 154: 19–29, 2006a.
- Frederickson CJ, Giblin LJ, Krezel A, McAdoo DJ, Muelle RN, Zeng Y, Balaji RV, Masalha R, Thompson RB, Fierke CA, Sarvey JM, de Valdenebro M, Prough DS, Zornow MH.** Concentrations of extracellular free zinc (pZn)(e) in the central nervous system during simple anesthesia, ischemia and reperfusion. *Exp Neurol* 198: 285–293, 2006b.
- Frederickson CJ, Koh JY, Bush AI.** The neurobiology of zinc in health and disease. *Nat Rev Neurosci* 6: 449–462, 2005.
- Frederickson CJ, Suh SW, Silva D, Frederickson CJ, Thompson RB.** Importance of zinc in the central nervous system: the zinc-containing neuron. *J Nutr* 130: 1471S–1483S, 2000.
- Fuentealba P, Timofeev I, Bazhenov M, Sejnowski TJ, Steriade M.** Membrane bistability in thalamic reticular neurons during spindle oscillations. *J Neurophysiol* 93: 294–304, 2005.
- Gibbs JW 3rd, Zhang YF, Shumate MD, Coulter DA.** Regionally selective blockade of GABAergic inhibition by zinc in the thalamocortical system: functional significance. *J Neurophysiol* 83: 1510–1521, 2000.
- Harris RJ, Symon L, Branston NM, Bayhan M.** Changes in extracellular calcium activity in cerebral ischemia. *J Cereb Blood Flow Metab* 1: 203–9, 1981.
- Harrison NL, Gibbons SJ.** Zn<sup>2+</sup>: an endogenous modulator of ligand- and voltage-gated ion channels. *Neuropharmacology* 33: 935–952, 1994.
- Heinemann U, Louvel J.** Changes in [Ca<sup>2+</sup>]<sub>o</sub> and [K<sup>+</sup>]<sub>o</sub> during repetitive electrical stimulation and during pentetrazol induced seizure activity in the sensorimotor cortex of cats. *Pfluegers* 398: 310–317, 1983.
- Heinemann U, Lux HD, Gutnick MJ.** Extracellular free calcium and potassium during paroxysmal activity in the cerebral cortex of the cat. *Exp Brain Res* 27: 237–243, 1977.
- Hille B.** *Ionic Channels of Excitable Membranes*. Sunderland, MA: Sinauer, 1992.
- Hines ML, Carnevale NT.** The NEURON simulation environment. *Neural Comput* 9: 1179–1209, 1997.
- Hodgkin AL, Huxley AF.** A quantitative description of membrane current and its application to conduction and excitation in nerve. *J Physiol* 117: 500–544, 1952.
- Horning MS, Trombley PQ.** Zinc and copper influence excitability of rat olfactory bulb neurons by multiple mechanisms. *J Neurophysiol* 86: 1652–1660, 2001.
- Howell GA, Welch MG, Frederickson CJ.** Stimulation-induced uptake and release of zinc in hippocampal slices. *Nature* 308: 736–738, 1984.
- Huguenard JR, Prince DA.** A novel T-type current underlies prolonged Ca<sup>2+</sup>-dependent burst firing in GABAergic neurons of rat thalamic reticular nucleus. *J Neurosci* 12: 3804–3817, 1992.
- Jeong SW, Park BG, Park JY, Lee JW, Lee JH.** Divalent metals differentially block cloned T-type calcium channels. *Neuroreport* 14: 1537–1540, 2003.
- Jokovic PM, Bayliss DA, Todorovic SM.** Different kinetic properties of two T-type Ca<sup>2+</sup> currents of rat reticular thalamic neurons and their modulation by enflurane. *J Physiol* 566: 125–142, 2005a.
- Jokovic PM, Brimelow BC, Murbartian J, Perez-Reyes E, Todorovic SM.** Contrasting anesthetic sensitivities of T-type Ca<sup>2+</sup> channels of reticular thalamic neurons and recombinant Ca(v) 3.3 channels. *Br J Pharmacol* 144: 59–70, 2005b.
- Kay AR.** Evidence for chelatable zinc in the extracellular space of the hippocampus but little evidence for synaptic release of Zn. *J Neurosci* 23: 6847–6855, 2003.
- Khosravani H, Altier C, Simms B, Hamming KS, Snutch TP, Mezeyova J, McRory JE, Zamponi GW.** Gating effects of mutations in the Cav3.2 T-type calcium channel associated with childhood absence epilepsy. *J Biol Chem* 279: 9681–9684, 2004.
- Kostyuk PG, Shuba Ya M, Savchenko AN.** Three types of calcium channels in the membrane of mouse sensory neurons. *Pfluegers* 411: 661–669, 1988.
- Kozlov AS, McKenna F, Lee JH, Cribbs LL, Perez-Reyes E, Feltz A, Lambert RC.** Distinct kinetics of cloned T-type Ca<sup>2+</sup> channels lead to differential Ca<sup>2+</sup> entry and frequency dependence during mock action potentials. *Eur J Neurosci* 11: 4149–4158, 1999.
- Lee JH, Daud AN, Cribbs LL, Lacerda AE, Pereverzev A, Klockner U, Schneider T, Perez-Reyes E.** Cloning and expression of a novel member of the low voltage-activated T-type calcium channel family. *J Neurosci* 19: 1912–1921, 1999.
- Mathie A, Sutton GL, Clarke CE, Veale EL.** Zinc and copper: pharmacological probes and endogenous modulators of neuronal excitability. *Pharmacol Ther* 111: 567–583, 2006.
- Matias CM, Matos NC, Arif M, Dionisio JC, Quinta-Ferreira ME.** Effect of the zinc chelator *N,N,N',N'*-tetrakis (2-pyridylmethyl)ethylenediamine (TPEN) on hippocampal mossy fiber calcium signals and on synaptic transmission. *Biol. Res.* 39: 521–530, 2006.
- McCormick DA, Huguenard JR.** A model of the electrophysiological properties of thalamocortical relay neurons. *J Neurophysiol* 68: 1384–1400, 1992.
- Mengual E, Casanovas-Aguilar C, Perez-Clausell J, Gimenez-Amaya JM.** Thalamic distribution of zinc-rich terminal fields and neurons of origin in the rat. *Neuroscience* 102: 863–884, 2001.
- Murbartian J, Arias JM, Perez-Reyes E.** Functional impact of alternative splicing of human T-type Cav3.3 calcium channels. *J Neurophysiol* 92: 3399–3407, 2004.
- Noh JH, Chung JM.** Zinc reduces low-threshold Ca<sup>2+</sup> currents of rat thalamic relay neurons. *Neurosci Res* 47: 261–5, 2003.
- Perez-Reyes E.** Molecular physiology of low-voltage-activated t-type calcium channels. *Physiol Rev* 83: 117–161, 2003.
- Perez-Reyes E, Cribbs LL, Daud A, Lacerda AE, Barclay J, Williamson MP, Fox M, Rees M, Lee JH.** Molecular characterization of a neuronal low-voltage-activated T-type calcium channel. *Nature* 391: 896–900, 1998.
- Qian J, Noebels JL.** Visualization of transmitter release with zinc fluorescence detection at the mouse hippocampal mossy fiber synapse. *J Physiol* 566: 747–758, 2005.
- Raymond V, Laped B.** Hyperpolarization-activated inward potassium and calcium-sensitive chloride currents in beating pacemaker insect neurosecretory cells (dorsal unpaired median neurons). *Neuroscience* 93: 1207–1218, 1999.
- Shuba YM, Teslenko VI, Savchenko AN, Pogorelaya NH.** The effect of permeant ions on single calcium channel activation in mouse neuroblastoma cells: ion-channel interaction. *J Physiol* 443: 25–44, 1991.
- Steriade M.** Sleep, epilepsy and thalamic reticular inhibitory neurons. *Trends Neurosci* 28: 317–24, 2005.
- Steriade M, McCormick DA, Sejnowski TJ.** Thalamocortical oscillations in the sleeping and aroused brain. *Science* 262: 679–85, 1993.
- Talavera K, Janssens A, Klugbauer N, Droogmans G, Nilius B.** Pore structure influences gating properties of the T-type Ca<sup>2+</sup> channel alpha1G. *J Gen Physiol* 121: 529–540, 2003.
- Talley EM, Cribbs LL, Lee JH, Daud A, Perez-Reyes E, Bayliss DA.** Differential distribution of three members of a gene family encoding low voltage-activated (T-type) calcium channels. *J Neurosci* 19: 1895–1911, 1999.
- Thompson RB, Whetsell WO, Jr, Maliwal BP, Fierke CA, Frederickson CJ.** Fluorescence microscopy of stimulated Zn(II) release from organotypic cultures of mammalian hippocampus using a carbonic anhydrase-based biosensor system. *J Neurosci Methods* 96: 35–45, 2000.
- Traboulsie A, Chemin J, Chevalier M, Quignard JF, Nargeot J, Lory P.** Subunit-specific modulation of T-type calcium channels by zinc. *J Physiol* 578: 159–171, 2007.
- Tsien RW, Lipscombe D, Madison DV, Bley KR, Fox AP.** Multiple types of neuronal calcium channels and their selective modulation. *Trends Neurosci* 11: 431–438, 1988.
- Ueno S, Tsukamoto M, Hirano T, Kikuchi K, Yamada MK, Nishiyama N, Nagano T, Matsuki N, Ikegaya Y.** Mossy fiber Zn<sup>2+</sup> spillover modulates heterosynaptic *N*-methyl-D-aspartate receptor activity in hippocampal CA3 circuits. *J Cell Biol* 158: 215–220, 2002.
- Vitko I, Chen Y, Arias JM, Shen Y, Wu XR, Perez-Reyes E.** Functional characterization and neuronal modeling of the effects of childhood absence epilepsy variants of CACNA1H, a T-type calcium channel. *J Neurosci* 25: 4844–4855, 2005.
- Wu J, Ellsworth K, Ellsworth M, Schroeder KM, Smith K, Fisher RS.** Abnormal benzodi-azepine and zinc modulation of GABA<sub>A</sub> receptors in an acquired absence epilepsy model. *Brain Res* 1013: 230–240, 2004.
- Yue BW, Huguenard JR.** The role of H-current in regulating strength and frequency of thalamic network oscillations. *Thalamus Related Syst* 1: 95–103, 2001.